PROGRAM 1017

## Modal Analysis of Structures Using the Eigenvalue Technique

The purpose of this program is three-fold:

1. To calculate the mass and stiffness matrices associated with the structural model.
2. To determine the undamped natural periods of the model.
3. To calculate the maximum modal responses of the structure i.e. deflections, shears, and moments.

The stiffness and mass matrices may be required in order to perform a dynamic analysis of the structure. The maximum modal responses may be used to perform a spectral analysis.

The program has the following options:

1. Vertical translation.
2. Torsional modes.
3. Soil-structure interaction.
4. Liquid sloshing.
5. Direct introduction of stiffness and mass matrices.

## Solution of the Problem

The equations of motion describing the lumped mass system having n degrees of freedom are

$$[M]\{\ddot{x}\} + [C]\{\dot{x}\} + [K]\{x\} = \{P\} \qquad (1)$$

where

$[M]$ = the mass matrix (n x n)
$[C]$ = the damping matrix (n x n)
$[K]$ = the stiffness matrix (n x n)

It has been shown that for certain types of damping or, for moderate amounts of damping, the maximum response can be obtained from a study of the free vibrations of the structure[1]

$$[M]\{\ddot{x}\} + [K]\{x\} = \{0\} \qquad (2)$$

Assume

$$\{x\} = \{\phi\} \sin \omega t$$

Thus

$$\{-\omega^2 [M] + [K]\}\{\phi\} = \{0\} \qquad (3)$$

and for a solution to exist

$$|-\omega^2 [M] + [K]| = 0 \qquad (4)$$

| | | | | | | |
|---|---|---|---|---|---|---|
| SUBJECT PROGRAM 1017 | MADE BY REA | CHKD BY | REV | By | | CHARGE NO. 72.4333 |
| PROGRAM DESCRIPTION | DATE 10-9-71 | DATE 10-11-71 | | Chkd | | CD-6 |
| | | | | Date | | SHT ___ OF |

Expanding the determinant given in (4) and solving the resulting equation yields solutions for $w^2$. These solutions are the eigenvalues of the system. The periods of the structure are obtained using the following relationship

$$T_i = \frac{2\pi}{w_i} \qquad i = 1,n$$

Hence, a n degree of freedom structure has n natural periods of vibration.

After the eigenvalues are obtained, the maximum displacements for each mode are calculated using equation (3). Since the solution of these equations is not unique, all of the mass point displacements must be determined in relation to each other. This is done for all of the modes, yielding n deflection patterns. Note that all of the displacements in any individual mode have the correct relationship to each other while there is as yet no relationship between the magnitudes of the various mode shapes.

The n x n matrix having the displacements for each mode shape contained in its columns is called the eigenvector array ($\phi$).

In order to relate the mode shapes to each other, it is necessary to calculate a participation factor for each mode.

The undamped equation of motion is

$$[M]\,|\ddot{X}| + [K]\,|X| = |P_i| \qquad (5)$$

Assume that

$$|X_i| = [\phi_{im}]\,|u_m| \qquad i = 1,2,3,\ldots,n \qquad (6)$$

m = mode number

Substituting (6) into (5) and also premultiplying each side by $[\phi_{im}]^T$ yields[2]

$$\cancel{[M_m]}\,|\ddot{u}_m| + \cancel{[K_m]}\,|u_m| = |P_m| \qquad (7)$$

where

$$\cancel{[M_m]} = [\phi_{im}]^T\,[M]\,[\phi_{im}] \qquad (7a)$$

$$\cancel{[K_m]} = [\phi_{im}]^T\,[K]\,[\phi_{im}] \qquad (7b)$$

$$|P_m| = [\phi_{im}]^T\,|P_i| \qquad (7c)$$

Thus, we now have n uncoupled equations of the form

$$M_m\ddot{u}_m + K_m u_m = P_m$$

or

$$\ddot{u}_m + w^2_m u_m = \frac{P_m}{M} \qquad (8)$$

For earthquake loading

$$\{p_j\} = -\{m_i\}\ddot{u}_g \tag{9}$$

$\ddot{u}_g$ = earthquake acceleration

$\{m_i\}$ = column mass matrix consisting of mass terms which would be multiplied by incident acceleration if forced vibrations were being considered.

The general solution of eqn (8) i.e. the response of the nth mode is given by the Duhamel Integral

$$u_n(t) = \int_0^t \frac{p_n}{K_n \omega_n} \sin \omega_n (t-\tau) d\tau \tag{10}$$

Substituting (9) into (10) and using (7c) yields

$$u_n = u_n(t) = -\frac{\{\phi_{in}\}^T\{m_i\}}{K_n \omega_n} \int_0^t \ddot{u}_g(\tau) \sin \omega_n (t-\tau) d\tau \tag{11}$$

Now

$$S_{an} = \left[\omega_n \int_0^t \ddot{u}_g(\tau) \sin \omega_n (t-\tau) d\tau\right]_{max} \tag{12}$$

where $S_{an}$ is the spectral acceleration for the period associated with the $n^{th}$ mode.

Substituting (12) into (11)

$$(u_n)_{max} = -\frac{\{\phi_{in}\}^T\{m_i\}}{K_n \omega_n^2} S_{an} \tag{13}$$

Since $S_{Dn} = S_{an}/\omega^2$ where $S_{Dn}$ is the spectral displacement

$$(u_n)_{max} = -\frac{\{\phi_{in}\}^T\{m_i\}}{K_n} S_{Dn} \tag{14}$$

Using (7a) and (14) yields

$$(u_n)_{max} = -\frac{\{\phi_{in}\}^T\{m_i\}}{\{\phi_{in}\}^T\{m_i\}\{\phi_{in}\}} S_{Dn} \tag{15}$$

Therefore, eqn (15) yields the "participation" or "scale" factor $\gamma_n$ for each mode.

$$\gamma_n = \frac{\{\phi_{in}\}^T\{m_i\}}{\{\phi_{in}\}^T\{m_i\}\{\phi_{in}\}} \tag{16}$$

Assuming $S_{Dn}$ is the desired maximum response for a particular mode.

$$\alpha_m = \gamma_m \alpha\phi_m S_{Dm}$$

where $\alpha\phi_m$ is the response based upon the eigenvectors of the mode obtained by eqn (3).

The next step that is necessary is to obtain the maximum total response by combining the responses of the various modes. Since only rarely do all the modal responses obtain their maximum at the same time, some judgment must be exercised. An envelope of maximum response can be obtained by direct addition of all of the modal responses. However, in some cases, especially when there are a large number of degrees of freedom this method may be grossly conservative. A more accurate method would probably be by combining the modal responses by the "square root of the sum of the squares" method.

As a check on the solution for the eigenvectors, the dot product of the eigenvectors weighted with the mass matrix are calculated by the program.

$$\cos\beta = \frac{\left\{\phi_r\right\}^T [M] \left\{\phi_s\right\}}{\left\{\phi_r\right\} [M] \left\{\phi_s\right\}} \qquad r \neq s \qquad (17)$$

It can be shown that the eigenvectors are orthogonal and therefore[2]

$$\cos\beta = 0$$

## References

1. Blume, Newmark, & Corning, Design of Multistory Reinforced Concrete Buildings for Earthquake Motions, Portland Cement Association, 1961.

2. Hurty & Rubinstein, Dynamics of Structures, Prentice Hall, 1964.

Note:

An option has been added to the program to obtain the maximum total response. This is done by direct addition of the contribution of each mode the user wants to consider. (See input data cards 14 and 15).

# PROGRAM 1044

## SEISMIC ANALYSIS OF VESSEL APPENDAGES

Appendages to a vessel may not significantly contribute structurally to the dynamic responses of a model of a vessel. However, appendages can affect the vessel locally by vibrating differently from the model of the vessel at the point of attachment.

The response spectrum method of analysis is not a strictly adequate way of obtaining the maximum appendage accelerations since it does not include the possible consequences of near resonance between the vessel model and the appendage model.

This paper describes the method used to evaluate the maximum elastic differential accelerations between an independently vibrating appendage model and an elastic beam vessel model at the appendage elevation due to known excitations of the elastic beam model.

The method involves two distinct steps. Firstly, the necessary time-absolute acceleration records are computed at appendage elevations due to model excitations. Secondly, the maximum differential accelerations between each appendage model and the vessel model at the appendage elevation are obtained.

The time-absolute acceleration records at the appendage elevation are computed by use of a step-by-step matrix analysis procedure. The equations of motion for the vessel model are of the form:

$$[M]\{\ddot{u}\} + (\Delta T/\pi)[K]\{\dot{u}\} + [K]\{u\} = -[M]\{\ddot{u}_g\}$$

where

[M] = Mass matrix, order n x n, obtained from a modal analysis.

[K] = Stiffness matrix, order n x n, obtained from a modal analysis.

A = Portion of first mode critical damping for the model.

T = First mode period of the model.

[M] = A diagonal matrix, order n x n, with diagonal elements corresponding to elements of the mass matrix excited by translational accelerations.

$|\ddot{u}|$ = n x 1 matrix of relative accelerations between the model base and the n degress of freedom.

$|\dot{u}|$ = n x 1 matrix of velocities corresponding to $|\ddot{u}|$

$|u|$ = n x 1 matrix of displacements corresponding to $|\ddot{u}|$.

$|\ddot{u}_g|$ = n x 1 matrix of translation base acceleration.

n = Degrees of freedom of vessel model.

By taking a small time increment (smaller than the smallest perio. obtained from the modal analysis) and letting accelerations vary linearly within the selected increment, the equations of motion can be integrated for the quantities $\{u\}$, $\{\dot{u}\}$, and $\{\ddot{u}\}$ over the selected time increment.[1] The values obtained are superimposed upon the valuos of these quantities existing at the beginning of the time increment. This process is repeated for the duration of the excitation. The time-absolute acceleration records for each translational degree of freedom are the sums of $\{\ddot{u}\}$ and $\{\ddot{u}_g\}$ taken throughout the history of the excitation.

The second step is similar to the first step. The equation of motion (n = 1) is written for the appendage as a single degree-of-freedom elastic model using the time-absolute acceleration record obtained in step 1 at the appendage elevation as the excitation. This equation is solved in the same manner used in step 1. The maximum absolute value of $\{\ddot{u}\}$ obtained is the quantity desired. It is the maximum differential acceleration between the appendage model and the vessel model due to a known excitation of the vessel mod:

For any appendage, this two-step procedure should be executed three times. This is required to evaluate normal, tangential and vertical appendage accelerations with respect to a vessel cross-section.

[1] Wilson & Clough, Dynamic Response by Step-By-Step Matrix Analysis

# PROGRAM E1622

## LOAD GENERATION PREPROCESSOR FOR PROGRAM E1374

In order to perform non-axisymmetric analyses on shells, the load must often be defined using Fourier series representation. The purpose of Prog. E1622 is to calculate and store on magnetic tape a time history of the Fourier pressure amplitudes. The format of this tape is designed specifically for use with Program E1374.

The input consists primarily of pressure versus angle versus time data at user supplied elevations. An option of the program enables the TVA furnished data cards for the Watts Bar Containment to be used directly. The pressures given on these cards can be scaled by a factor input by the user.

The program plots the unscaled input pressure versus time for each shell compartment.

In order to calculate the amplitudes of the harmonics, a linear function in the circumferential direction is assumed between given points. (See Figure 1).

The output for user specified time steps will be written on a labeled tape or disk file assigned by the user. Printed output consists of the Fourier amplitudes at every time step plus the total number of timesteps for each harmonic.

| SUBJECT | MADE BY | CHKD BY | | BY | | CHART NO. |
|---|---|---|---|---|---|---|
| PROGRAM E1622 DESCRIPTION | CJP | FPS | | | | 72-433 |
| | DATE 10/73 | DATE 10/73 | | DATE | | CBI |

Other features and assumptions of the program are:

1. Only distributed loads are considered.

2. The model consists of a cylindrical shell and optional hemispherical top head.

3. The pressure has a block type distribution in the longitudinal direction. (See Fig. 1)

4. Any initial pressure acting on the shell can be subtracted from the input pressure histories.

5. Amplitudes for both sine and cosine terms can be calculated with the user supplying the range of harmonics to be output.

CBB

Location _____

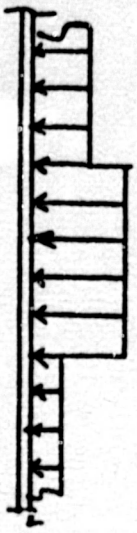

ASSUMED SHAPE OF
PRESSURE DISTRIBUTION
IN LONGITUDINAL DIRECTION

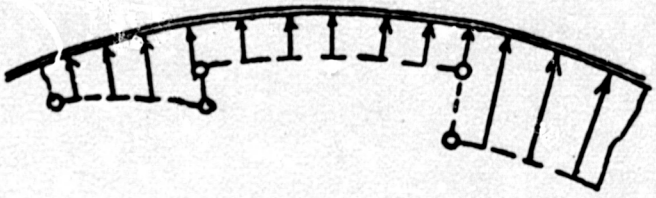

ASSUMED SHAPE IN
CIRCUMFERENTIAL DIRECTION

o GIVEN POINTS

--- GENERATED BY PROGRAM E162

$$p(x,\theta,t) = \sum_{n=0}^{m} p_n(x,t)\cos n\theta + \sum_{j=1}^{m} p_j(x,t)\sin j\theta$$

where

$$p_0(x,t) = \frac{1}{2\pi}\int_0^{2\pi} p(x,\theta,t)\,d\theta$$

$$p_n(x,t) = \frac{1}{\pi}\int_0^{2\pi} p(x,\theta,t)\cos n\theta\,d\theta \qquad n \geq 1$$

$$p_j(x,t) = \frac{1}{\pi}\int_0^{2\pi} p(x,\theta,t)\sin j\theta\,d\theta \qquad n \geq 1$$

$x$ = LONGITUDINAL COORDINATE
$\theta$ = AZIMUTH
$t$ = TIME
$m$ = TOTAL NUMBER OF CIRCUMFERENTIAL WAVES

| SUBJECT: PROGRAM E162 | MADE BY: CAP | CHKD BY: | REV | By | | CHARGE NO. 77-4333 |
|---|---|---|---|---|---|---|
| FIG. 1 | DATE: 10/11/77 | DATE: 10/11/77 | | Chkd | | |
| | | | | Date | | SHT C820 OF |

# PROGRAM E1623

## POST-PROCESSOR PROGRAM FOR PROGRAM E1374

Program E1623 was written specifically for the TVA Watts Bar Containment Vessels. It performs the following operations:

1. Using Fourier data generated by Program E1374 (Dynamic Shell Analysis), the summed displacements, forces and stresses found for various points around the shell circumference at each output point on the meridian.

2. The maximum of the summed values along with the associated time and azimuth are saved for each elevation and printed out at the end of the problem.

3. The following tables are printed:
   1. Radial deflection w at each elevation versus azimuth
   2. Longitudinal force $N_\phi$ at each elevation versus azimuth
   3. Longitudinal moment $M_\phi$ at each elevation versus azimuth
   4. Circumferential force $N_{\phi\theta}$ at each elevation versus azimuth

The time basis for these tables is the occurrence of the minimum longitudinal force at the base.

4. Ring forces are calculated using the equations shown in this writeup and then the maximums are pointed out.

5. Displacement traces at several elevations can be saved on a tape or disk unit.

6. The membrane stress resultants are saved on either a tape or disk unit for input into the buckling check program.

Program E1374 writes the Fourier amplitude results of the fundamental variables (w, $u_\phi$, $\beta_\phi$, $u_\theta$, Q, N$\phi$, M$\phi$, N) on a labeled tape after each timestep. Program E1623 reads this tape, interpolates to obtain the values at the output times, and calculates the remaining forces[1] and all the stresses.

The amplitudes are then summed using the following equation:

$$f(x,\theta,t) = \sum_{n=0}^{m} g(x,t)\text{Cosn}\theta + \sum_{n=1}^{m} h_n(x,t)\text{Sinm}\theta$$

$x$ = meridianal coordinate
$t$ = time
$g_n(x,t)$ = amplitudes of cosine harmonics
$h_n(x,t)$ = amplitudes of sine harmonics
$\theta$ = azimuth
$f(x,0,t)$ = Fourier sum
$m$ = maximum number of circumferential waves

## CALCULATION OF RING LOADS

The assumptions used are:

1. One of the principal axes of the ring is parallel to the axis of rotation.
2. The ring is symmetric with respect to the principal axis which is perpendicular to the axis of rotation.
3. The shear center is at the centroid.

[1] See pg 472 of Ref. (1) for the equations used.

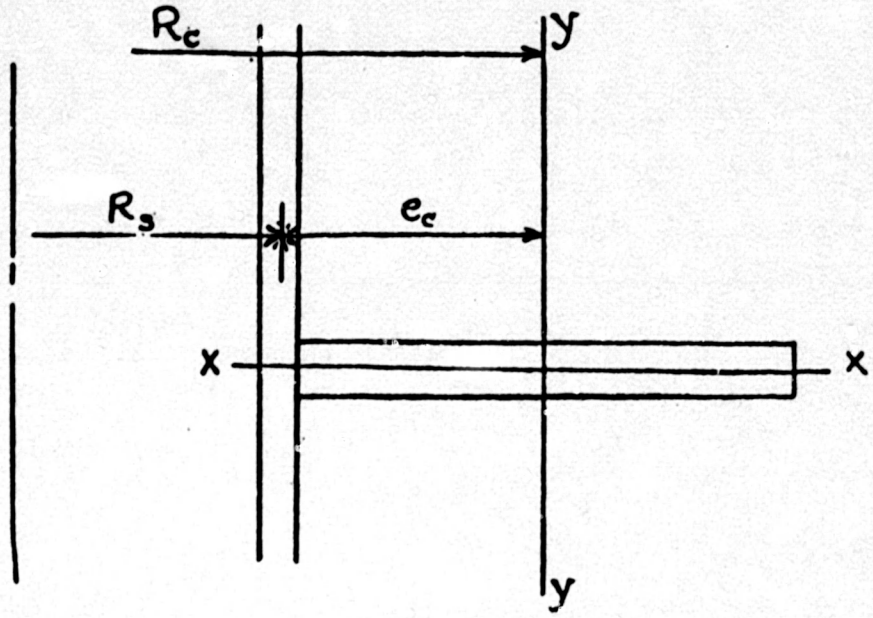


$W_r$ = radial displacement of ring

$V_r$ = tangential displacement of ring

$N_\theta$ = circumferential force in ring

$M_\theta$ = circumferential moment in ring

E = modulus of elasticity of ring

A = area of ring

I = moment of inertia of ring about y y

$W_s$ = radial displacement of shell

$V_s$ = tangential displacement of shell

$$V_r = V_s \left(1 + e_c / r_c\right) - e_c / r_c \dot{W}$$

$$W_r = W_s$$

$$N_\theta = \frac{EA}{r_c}\left(\dot{V}_r + W_r\right)$$

$$M_0 = \frac{EI}{r_c^2}\left(-\ddot{W}_r + \dot{V}_r\right)$$

| SUBJECT | MADE BY | CHKD BY | | | | CHANGE NO. |
|---|---|---|---|---|---|---|
| PROGRAM E1623 DESCRIPTION | CJP | FRS | | | | 72-4332 |
| | DATE 10/73 | DATE 10/73 | | | | SHT CB 23 OF |

Where a dot denotes differentiation with respect to the circumferential coordinate.

Weld shear - the weld shear equals the jump in shell in-plane shear at the ring.

# PROGRAM E1624

**SPCGEN - Spectral Curve Generation**

Program E1624 reads the Fourier amplitudes of the deflection transients stored on magnetic tape from the output of program E1374. The program then proceeds as follows to calculate the accelerations at uniform time intervals and to evaluate the response spectra:

1. From the deflection transient for each harmonic, the acceleration traces are computed using three point central difference for the first and last three time steps, and a seven point central difference elsewhere.

   a. Three point central difference equation:
   let $y = f(t)$ be the function that fits a data set, then a three point central difference equation is:

$$\left(\frac{d^2y}{dt^2}\right)_i = \frac{1}{h^2}\left(y_{i+1} - 2y_i + y_{i-1}\right)$$

   where,
   $y_{i+1} = f(t_{i+1})$, $y_i = f(t_i)$, and $y_{i-1} = f(t_{i-1})$

   are three consecutive displacements in the data set at equal time intervals h, where $h = t_{i+1} - t_i = t_i - t_{i-1}$

   b. Seven point central difference equation:
   The seven point central difference equation, using Stirling's formula at $t = t_i$, is:

$$\left(\frac{d^2y}{dt^2}\right)_i = \frac{1}{180h^2}\Big[\, 2\left(y_{i+3} + y_{i-3}\right) - 27\left(y_{i+2} + y_{i-2}\right) + 270\left(y_{i+1} + y_{i-1}\right) - 490y_i \,\Big]$$

where, $y_{i+3} = f\left(t_{i+3}\right)$, $y_{i+2} = f\left(t_{i+2}\right)$, etc....

and h is as defined above.

2. The Fourier amplitudes of the acceleration transient for each harmonic obtained in step 1 are interpolated to obtain a common timestep.

3. The accelerations of step 2 are summed for given angles:

$$\left(\frac{d^2y}{dt^2}\right)_{\theta\theta} = \sum_{n=1}^{n=k} A_n \sin n\theta + \sum_{n=0}^{n=j} B_n \cos n\theta$$

where,

n = number of circumferential waves (harmonic number)

k = number of sine harmonics

j = number of cosine harmonics

4. CBI program E1668 is now used as a subroutine to evaluate the dynamic response spectra and present the results on printed plots. A brief description of this program follows.

CBI

Location Birmingham

# Description of Program E1391Ø

## Shell Buckling Analysis for TVA Containment Vessel

### Introduction

Program #1391Ø performs the buckling check of the TVA ice condenser containment vessel for Non-axisymmetric pressure loading combining with the dead loads and seismic loads occuring in the vessel. The non-axisymmetric loads are developed by CBI program E1374. The resulting stresses are compared to critical buckling stress and by using a specified factor of safety the buckling ratio is found.

### Calculation of Dead Loads and Seismic Loads

As a general rule, dead loads and seismic loads are calculated at a few points along the vessel and the vessel is checked for buckling at many more points. As a result the program performs a linear interpolation to derive the dead loads and seismic loads at any given point along the vessel.

### Calculation of Critical Buckling Stresses

In order to determine the critical buckling stress at a given point it is necessary to determine the geometry in the region of that point. The program considers four cases:

a) cylinders stiffened meridionally and circumferentially
b) cylinders stiffened circumferentially
c) spheres stiffened circumferentially and meridionally
d) unstiffened spheres

For each of these conditions certain constants must be determined based on known geometry. This information is in the form of graphs and is input into the computer as a series of straight lines. Once these constants are known, the critical buckling stresses can be determined using the applicable formulae. These calculations are based on Appendix H of TVA specification 1440.

## PROGRAM E1668

**SPECTR - Spectral Analysis for Acceleration Records Digitized at Equal Intervals**

Program E1668 evaluates dynamic response spectra at various periods and presents the results on a printed plot. Given the time-acceleration record, the program numerically integrates the normal convolution time integral for various natural periods and damping ratios. The computed relative displacements, relative and pseudo-relative velocities, and absolute and pseudo-absolute accelerations are tabulated for periods from 0.025 seconds to 1 second.

### Mathematical Formulation

For a single degree of freedom system, the equation of motion is

$$m\ddot{x} + c\dot{x} + kx = -m\ddot{s}(t) \qquad (1)$$

where m, c, and k are the mass, damping, and stiffness, respectively.

Dividing by m, the following equation is obtained.

$$\ddot{x} + 2\beta\omega\dot{x} + \omega^2 x = -\ddot{s}(t) \qquad (2)$$

$\beta$ = percentage of critical damping
$\omega$ = circular frequency

the solution of Eq. (2) is

$$x(t) = c(t) - A(t) \qquad (3)$$

CBI

Description of Program E13910 cont.

Location Birmingham

Calculation of Stress and Buckling Ratios

The program calculates stresses and buckling ratios at any number of elevations and azimuths and for any number of time periods and then finds the maximum buckling ratio at each elevation. The program calculates four stresses at each point:

a) meridional stress due to axial loads
b) meridional stress due to bending loads
c) circumferential stress
d) shear stress

The program considers only compressive stresses. If a stress is tensile it is set equal to zero. For each of the stresses a buckling ratio is calculated using the stress multiplied by a factor of safety and divided by the critical buckling stress. These buckling ratios are then combined and five ratios result:

a) Axial + Circumferential
b) Axial + Bending
c) Axial + Shear
d) Axial + Shear + Bending
e) Axial + Shear + Circumferential

After these combined ratios are calculated, the maximums regardless of time or azimuth are recorded for each elevation.

In areas where vertical stiffening is present the program calculates the buckling ratio of the stiffener acting with the shell as a column simply supported at each end. The portion of the shell used in the column is determined using the rules of the Shell Analysis Manual referenced in Appendix H of Specification 1440. The buckling ratio is calculated in the manner discussed previously and the maximum is recorded.

Program Output

The program prints out the following data at each elevation considered:

a) Basic shell data and geometry of stiffeners
b) Load such as static pressure, dead loads, and seismic loads
c) Buckling stress coefficient
d) The five combined buckling ratios.
e) Vertical stiffener buckling ratios

where

$$c(t) = e^{-\beta\omega t}\left(\frac{\dot{x}_o + \beta\omega x_o}{\bar{\omega}} \sin(\bar{\omega}t) + x_o \cos(\bar{\omega}t)\right)$$

$$A(t) = \int_0^t \frac{1}{\bar{\omega}} e^{-\beta\omega(t-\tau)} \ddot{s}(\tau) \sin\left[\bar{\omega}(t-\tau)\right] d\tau$$

$$\bar{\omega} = \omega \ (1-\beta^2)$$

$\dot{x}_o$ and $x_o$ are the initial velocity and displacement respectively.

At any point in time during the acceleration trace, c(t) is re-evaluated such that the initial conditions are assumed to be the velocity and displacement obtained at the previous step. Thus, the integration for A(t) needs to be performed over only one timestep interval.

The relative velocity at each time is obtained by differentiating Eq. (3). Then Eq. (2) can be employed to determine the absolute acceleration.

The spectral values are then defined as the maximum values of x, $\dot{x}$, and $\ddot{x}$, occurring during the record. The pseudo-relative velocity and pseudo-absolute acceleration are then calculated using the following equations.

$$v = \omega x_{max}$$

$$a = \omega^2 x_{max}$$

## SHELL DESIGN

The Containment Vessel is designed for static internal pressure loading in accordance with the ASME Boiler and Pressure Vessel Code, Section III, Nuclear Power Plant Components and Section VIII, Division 1, Pressure Vessels with Winter 1971 Addenda. The shell formulae used in determining the minimum required shell thicknesses are from Paragraph UG-27 of Section VIII and are shown below:

Circumferential Direction (Cylindrical Vessel)

$$t = \frac{PR}{SE - 0.6P}$$

Meridional Direction (Cylindrical Vessel)

$$t = \frac{PR}{2SE + 0.4P}$$

Spherical Shell

$$t = \frac{PR}{2SE - 0.2P}$$

where: t = minimum required shell thickness (inches)

P = internal pressure (psi)

R = vessel radius (inches)

S = Allowable Stress Value (psi)

E = Shell joint weld efficiency

Other portions of the Containment Vessel such as the penetrations and the personnel lock barrel are designed in accordance with the above rules as applicable.

The Containment Vessel shell and stiffener rings are designed in accordance with Paragraph UG-28 of Section VIII for external pressure.

The containment vessel is designed and analyzed for the non-axisymmetric pressure transient loads resulting from a loss-of-coolant accident in accordance with TVA Specification 1440. Stresses are limited to the allowable stress values stated in Section A of this Stress Report. In addition. a buckling analysis is performed to determine the stability of the vessel in accordance with Appendix H, Revision 1, of TVA Specification 1440. which is reprinted at the end of this section.

PENETRATIONS

The penetrations and reinforcement are proportioned in accordance with the rules presented in Paragraph NE-3330 of Section III. In addition, the penetration assemblies and surrounding shell of loaded penetrations are designed and analyzed in accordance with the rules presented in the Welding Research Council Bulletin Number 107. Permanent caps for spare penetrations are designed in accordance with Paragraph UG-34 of Section VIII. The flanges and bolted covers are designed in accordance with Appendix II of Section VIII.

ATTACHMENTS

Attachments to the Containment Vessel pressure boundary or to material required for the pressure retaining function are designed in accordance with the ASME Code, and the stresses are limited to that allowed by the ASME Code. These rules are applied to the attachment for a distance from the pressure retaining material of 16 times the attachment thickness or 4 inches, whichever is lesser. The remainder of the attachment and other items covered by this Stress Report are designed in accordance with the rules of the AISC Manual of Steel Construction, Seventh Edition.

BOTTOM LINER

Although the bottom liner is furnished by CBI, the design responsibility is by TVA. The rules of Section III of the ASME Code are not applicable.

## GENERAL REFERENCES

1. ASME Boiler and Pressure Vessel Code, 1971 Edition with Winter 1971 Addenda, including the following sections:

   a) Section II, Material Specifications

   b) Section III, Nuclear Power Plant Components

   c) Section VIII, Division 1, Pressure Vessels

2. Manual of Steel Construction, American Institute of Steel Construction, Seventh Edition.

3. John F. Harvey, Pressure Vessel Design, Van Nostrand, Princeton, New Jersey, 1963.

4. S. Timoshenko and S. Woinowsky - Krieger, Theory of Plates and Shells, McGraw-Hill, New York, Second Edition, 1959.

5. W. Flugge, Stresses in Shells, Springer-Verlag, Berlin, Germany, 1962.

6. S. Timoshenko. Theory of Elastic Stability", Engineering Societies Monograph, McGraw-Hill, New York, 1936.

7. O. Blodgett, Design of Welded Structures, The James F. Lincoln Arc Welding Foundation, Cleveland, Ohio, 1966.

8. K. R. Wichman, et.al, "Local Stresses in Spherical and Cylindrical Shells due to External Loadings", Welding Research Council, Bulletin Number 107, August, 1965.

9. Raymond J. Roark, Formulas For Stress and Strain, McGraw-Hill, New York, Fourth Edition, 1965.

10. E. M. Baker, et.al, Shell Analysis Manual, National Aeronautics and Space Administration, Washington, D.C., April, 1968.

11. A. Kalnins, "Analysis of Shells of Revolution Subjected to Symmetric and Non-Symmetric Loads", Transactions of the ASME Journal of Applied Mechanics, September, 1964.

12. M. Kraus, Thin Elastic Shells, John Wiley, New York, 1967.

13. A. Kalnins, "On Free and Forced Vibration of Rotationally Symmetric Layered Shells", Transactions of the ASME, Journal of Applied Mechanics, December, 1965.

14. W. C. Hurty and M. F. Rubenstein, Dynamics of Structures, Prentice-Hall, Englewood Cliffs, New Jersey, 1964.

15. J. C. Houbolt, "A Recurrence Matrix Solution For The Dynamic Response of Elastic Aircraft," J. Aero. Sci. 17, 1950.

16. L. E. Grinter Theory of Modern Steel Structures, Volume II, Macmillan, New York, 1949.

Subsection CE

# Computer Programs Used by Anamet

Anamet Lab. #1272.23C
December 23, 1972
Revised October 31, 1973

# PROGRAM BALL
# ANALYSIS OF NONLINEAR DYNAMIC SHELLS OF REVOLUTION

By

R. L. Citerley
R. E. Ball

Anamet Laboratories, Inc.
727 Industrial Road
San Carlos, California 94070

*Anamet Laboratories, Inc.*

P.O. BOX 831, SAN CARLOS, CALIFORNIA 94070

## TABLE OF CONTENTS

I INTRODUCTION . . . . . 1

II THEORY

A. Shell Geometry . . . . . 2
B. Strain-displacement Relations . . . . . 4
C. Equations of Motion . . . . . 6
D. Constituitive Relations . . . . . 7
E. Boundary Conditions . . . . . 9
F. Ring Stiffeners . . . . . 10

III METHOD OF SOLUTION

A. Fourier Expansions . . . . . 14
B. Modal Uncoupling . . . . . 14
C. Spatial Finite Difference Formulation . 16
D. Time-Wise Differencing . . . . . 19
E. Damping . . . . . 22
F. Solution by Elimination . . . . . 22
G. Poles . . . . . 24
H. Computer Program . . . . . 25

IV REFERENCES . . . . . 27

APPENDIX A - ELASTIC STATIC

APPENDIX B - BIFURCATION STATIC

APPENDIX C - NONLINEAR DYNAMIC

APPENDIX D - ELASTIC WITH RINGS-STATIC

APPENDIX E - ELASTIC ORTHOTROPIC DYNAMIC

APPENDIX F - FULL FOURIER EXPANSIONS

*Anamet Laboratories, Inc.*

P.O. BOX 631, SAN CARLOS, CALIFORNIA 94070

# I INTRODUCTION

The numerical analysis of thin shells of revolution is a subject that has received a considerable amount of attention in recent years. Most of this attention has been given to the linear analysis of symmetric and nonsymmetric loaded shells. The dynamic (transient) behavior of shells has also been given some attention. Little discussion has been presented for the static nonlinear behavior of a shell of revolution. Further, discussions on the nonlinear transient behavior of nonsymmetrically loaded shells are minimal.

Anamet and its consultants have illustrated the nonlinear dynamic behavior of isotropic shells of revolution.[1,2,3,4*] The purpose of this study is to report upon a nonlinear, dynamic shell of revolution computer program which permits the inclusion of circumferential rings. Sanders[5] nonlinear equations of equilibrium are used as the basis of this development. The constituitive relations used by Sanders are the same as Love's first approximation. A compatible set of equilibrium equations is derived for discrete circumferential rings and layered orthotropic shells. Program efficiency is attained by the described variable mesh spacing. The above features are provided in the BALL computer program. Even though the development is based upon a nonlinear theory, this program is applicable to linear, elastic, dynamic behavior of shells of revolution. The linear and nonlinear features of the BALL program are illustrated by a number of sample solutions. These results are compared to other published results.

* superscript numbers denote references.

## II THEORY

### A. Shell Geometry

Consider the general shell of revolution shown in figure 1. Located within this shell is a reference surface. All material points of the shell can be located using the orthogonal coordinate system $s$, $\theta$, $\zeta$, where $s$ is the meridional distance along the reference surface measured from one boundary, $\theta$ is the circumferential angle measured from a datum meridian plane, and $\zeta$ is the normal distance from the reference surface. Further, let the location of the reference surface be described by the dependent variable $r$, the normal distance from the axis of the shell. Accordingly, the principal radii of curvature of the reference surface are

$$R_\theta = r/[1 - (r')^2]^{\frac{1}{2}} \tag{1}$$

$$R_s = - [1 - (r')^2]^{\frac{1}{2}}/r'' \tag{2}$$

where a prime denotes differentiation with respect to $s$. Further, note the Codazzi identity

$$(\frac{1}{R_\theta})' = r' (R_s^{-1} - R_\theta^{-1})/r \tag{3}$$

and the relation

$$r'' = - r/R_s R_\theta \tag{4}$$

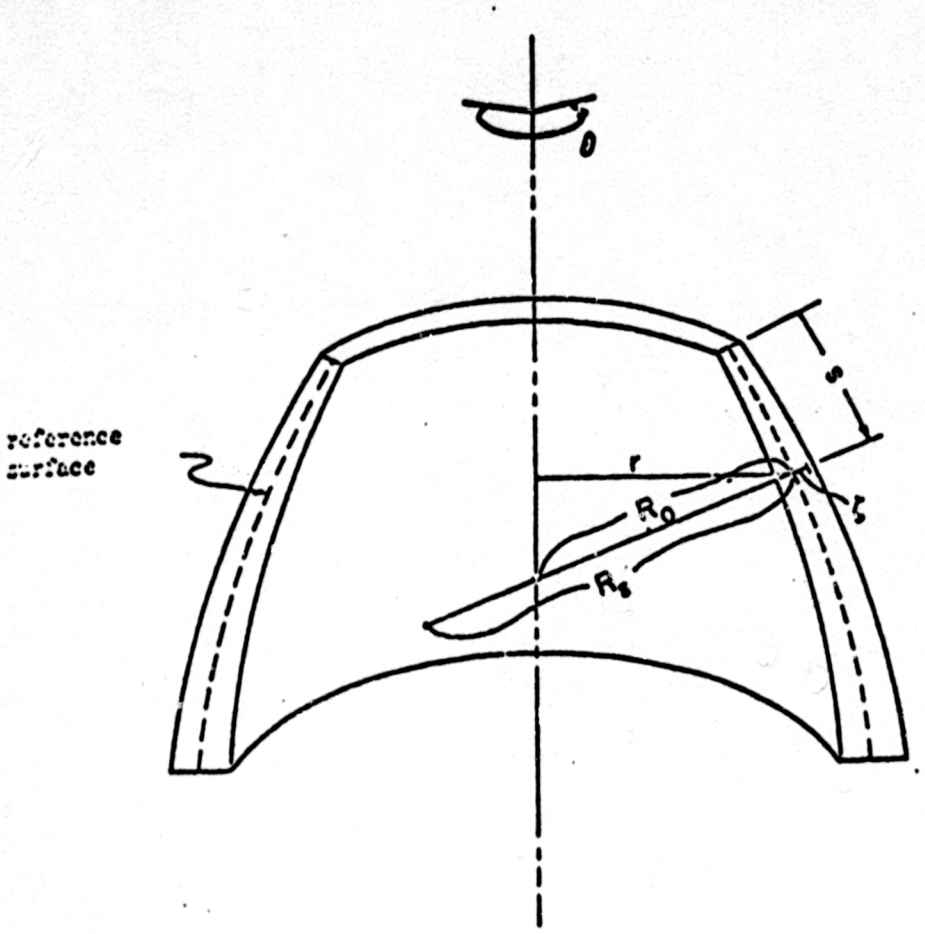


Figure 1. Shell Geometry and Coordinates



CE-5

B. Strain-displacement Relations

For a shell of revolution, the strain-displacement relations derived by Sanders[5] take the form

$$\left.\begin{aligned} \varepsilon_s &= U' + W/R_s + (\phi_s^2 + \phi^2)/2 \\ \varepsilon_\theta &= \dot{V}/r + r' U/r + W/R_\theta + (\phi_\theta^2 + \phi^2)/2 \\ \varepsilon_{s\theta} &= (V' + \dot{U}/r - r'V/r + \phi_s \phi_\theta)/2 \end{aligned}\right\} \quad (5)$$

$$\left.\begin{aligned} \kappa_s &= \phi_s' \\ \kappa_\theta &= \dot{\phi}_\theta/r + r' \phi_s/r \\ \kappa_{s\theta} &= [\phi_\theta' + \dot{\phi}_s/r - r' \phi_\theta/r + (R_\theta^{-1} - R_s^{-1}) \phi]/2 \end{aligned}\right\} \quad (6)$$

where $\varepsilon_s$, $\varepsilon_\theta$, and $\varepsilon_{s\theta}$ are the reference surface strains, $\kappa_s$, $\kappa_\theta$, and $\kappa_{s\theta}$ are the bending strains, U and V are displacements in the directions tangent to the meridian and to the parallel circle respectively, W is the displacement normal to the reference surface, and $\phi_s$, $\phi_\theta$, and $\phi$ are rotations defined by

$$\left.\begin{aligned} \phi_s &= - W' + U/R_s \\ \phi_\theta &= - \dot{W}/r + V/R_\theta \\ \phi &= (V' + r'V/r - \dot{U}/r)/2 \end{aligned}\right\} \quad (7)$$

In these equations, and henceforth, a superscript dot denotes differentiation with respect to $\theta$. The positive direction of each displacement and rotation variable is indicated in figure 2.

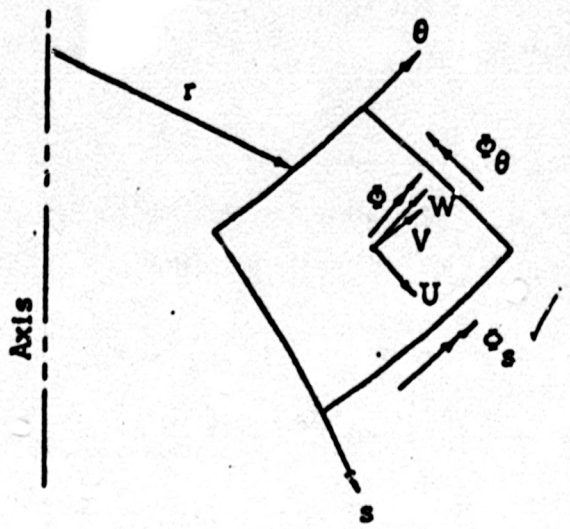


Figure 2. Positive Directions for Displacements and Rotations

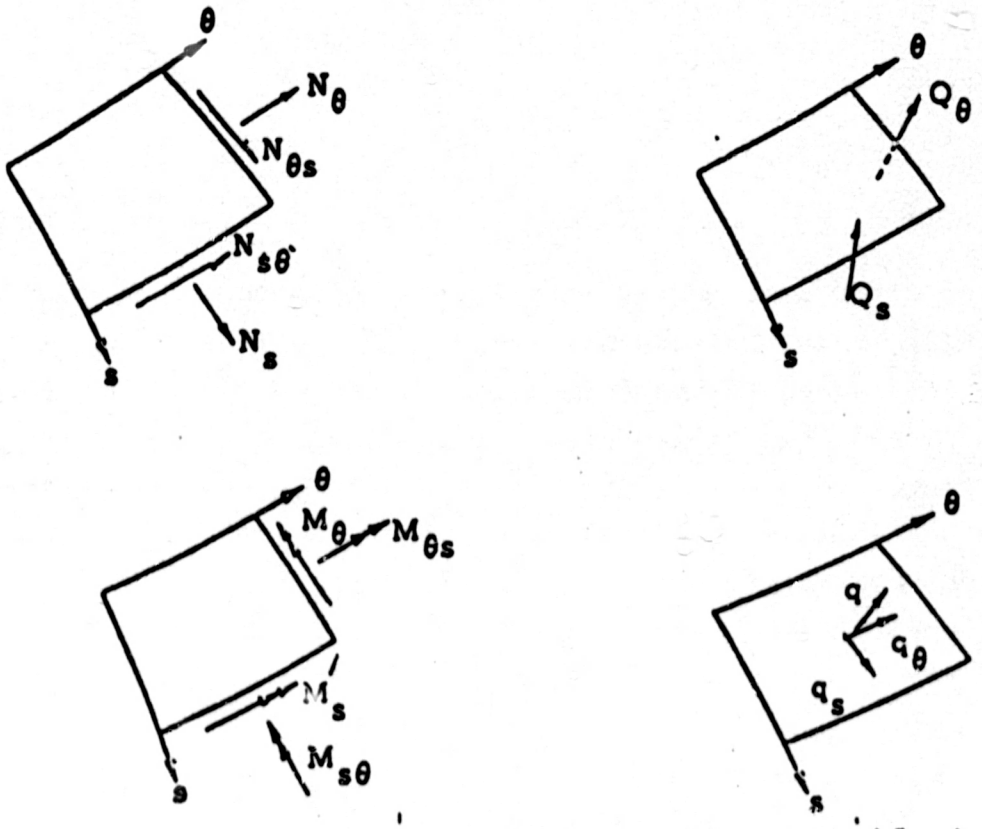


Figure 3. Positive Directions for Forces, Moments and Loads.



CE-1

C. Equations of Motion

Converting Sanders' equilibrium equations to the equations of motion for a shell of revolution leads to

$$\left.\begin{aligned}
&(rN_s)' + \dot{N}_{s\theta} - r'N_\theta + rQ_s/R_s + (R_s^{-1} - R_\theta^{-1})\,\dot{M}_{s\theta}/2 = r(\int m d\zeta)\partial^2 U/\partial T^2 \\
&- rq_s + \underline{r(\phi_s N_s + \phi_\theta N_{s\theta})/R_s} + \underline{[\phi(N_s + N_\theta)]^{\cdot}/2} \\
&\dot{N}_\theta + (rN_{s\theta})' + r'N_{s\theta} + rQ_\theta/R_\theta + r[(R_\theta^{-1} - R_s^{-1})M_{s\theta}]'/2 = \\
&r(\int m d\zeta)\partial^2 V/\partial T^2 - rq_\theta + \underline{r(\phi_\theta N_\theta + \phi_s N_{s\theta})/R_\theta} - \underline{r[\phi(N_s + N_\theta)]'/2} \\
&(rQ_s)' + \dot{Q}_\theta - rN_s/R_s - rN_\theta/R_\theta = r(\int m d\zeta)\partial^2 W/\partial T^2 \\
&- rq + \underline{(r\phi_s N_s + r\phi_\theta N_{s\theta})'} + \underline{(\phi_s N_{s\theta} + \phi_\theta N_\theta)^{\cdot}}
\end{aligned}\right\} \quad (8)^{*}$$

and

$$(rM_s)' + \dot{M}_{s\theta} - r'M_\theta - rQ_s = 0 \qquad (9)$$

$$\dot{M}_\theta + (rM_{s\theta})' + r'M_{s\theta} - rQ_\theta = 0 \qquad (10)$$

when the effects of rotary inertia are neglected. In equations (8) - (10), m is the mass density of the shell material, T is time, $q_s$, $q_\theta$, and q are the meridional, circumferential, and normal components of the applied pressure load, $Q_s$ and $Q_\theta$ are the transverse forces per unit length, $N_s$, $N_\theta$, and $N_{s\theta}$ are the membrane forces per unit length, and $M_s$, $M_\theta$, and $M_{s\theta}$ are the bending and twisting moments per unit length. Refer to Figure 3 for the positive directions of the pressure components, forces, and moments.

* underlined terms are the nonlinear terms

D. Constituitive Relations

The constitutive stress-strain-temperature relations assumed for the elastic behavior of the shell along the meridian are the following equations relating the force and moment resultants and strain and curvature expressions.

$$\begin{Bmatrix} N_s \\ N_\theta \\ N_{s\theta} \\ M_s \\ M_\theta \\ M_{s\theta} \end{Bmatrix} = \begin{bmatrix} C_{11} & C_{12} & 0 & K_{11} & K_{12} & 0 \\ C_{12} & C_{22} & 0 & K_{12} & K_{22} & 0 \\ 0 & 0 & C_{33} & 0 & 0 & K_{33} \\ K_{11} & K_{12} & 0 & D_{11} & D_{12} & 0 \\ K_{12} & K_{22} & 0 & D_{12} & D_{22} & 0 \\ 0 & 0 & K_{33} & 0 & 0 & D_{33} \end{bmatrix} \begin{bmatrix} e_s \\ e_\theta \\ e_{s\theta} \\ k_s \\ k_\theta \\ k_{s\theta} \end{bmatrix} + \begin{Bmatrix} C_{1T} \\ C_{2T} \\ 0 \\ D_{1T} \\ D_{2T} \\ 0 \end{Bmatrix} \quad (11)$$

Where

$$C_{ij} = \int B_{ij}\, d\zeta \quad (12a)$$

$$K_{ij} = \int B_{ij}\, \zeta\, d\zeta \quad (12b)$$

$$D_{ij} = \int B_{ij}\, \zeta^2\, d\zeta \quad (12c)$$

$$B_{ij} = \frac{E_{ij}}{1-\nu_i\nu_j} \text{ where } i = j = 1,2 \; ; \; B_{ij} = \frac{E_{ii}\,\nu_j}{1-\nu_i\,\nu_j}, \; i \neq j = 1,2 \quad (12d)$$

$$B_{ij} = 2G_{ij} \qquad \text{where } i, j = 3 \quad (12e)$$

$$C_{iT} = \int \alpha\, \tau\, E\, d\zeta \;/\; (1-\nu) \quad (12f)$$

$$D_{iT} = \int \zeta\, \alpha\, \tau\, E\, d\zeta \;/\; (1-\nu) \quad (12g)$$

In equations (12f) and (12g), $\tau$ is the local temperature change and $\alpha$ is the coefficient of thermal expansion.

The stiffness constants $C_{ij}$, $K_{ij}$, and $D_{ij}$, and the thermal forces and moments $C_{iT}$ and $D_{iT}$ are allowed to vary along the meridian. Equations (5) - (10) are 15 equations in terms of 15 unknowns $N_s$, $N_\theta$, $N_{s\theta}$, $M_s$, $M_\theta$, $M_{s\theta}$, $e_s$, $e_\theta$, $e_{s\theta}$, $k_s$, $k_\theta$, $k_{s\theta}$, $u_s$, $u_\theta$, w. They may be combined in many ways to eliminate some of the intermediate variables. One such procedure is to reduce the system of equations to four simultaneous second-order differential equations (the three equilibrium equations and the fourth of equations (8-11)) following the concepts of reference (6). As indicated in reference (6) $M_\theta$ must be eliminated in such a way that $k_s$ does not appear in order to prevent the appearance of derivatives of w higher than two. From the fourth and fifth of equations (11), the necessary relation can be obtained as

$$M_\theta = \frac{D_{12}}{D_{11}} M_s + \left[K_{12} - \frac{D_{12}\,K_{11}}{D_{11}}\right] e_s + \left[K_{22} - \frac{D_{12}\,K_{12}}{D_{11}}\right] e_\theta + \left[D_{22} - \frac{D_{12}^2}{D_{11}}\right] k_\theta + D_{2T} - \frac{D_{12}}{D_{11}} D_{1T} \tag{13}$$

and $u_s$, $u_\theta$, w, and $M_s$ are taken as the fundamental variables. The four simultaneous second-order differential equations can be written in matrix form as

$$Ez'' + Fz' + Gz + \bar{E}z'' + \bar{F}z' + \bar{G}z + E^*z'' + F^*z' + G^*z - \nu I\ddot{z} = e \tag{14}$$

where

$$z = \begin{Bmatrix} u_s \\ u_\theta \\ w \\ M_s \end{Bmatrix}, \quad \ddot{z} = \frac{\partial^2 z}{\partial t^2}, \quad I = \begin{bmatrix} 1 & 0 & 0 & 0 \\ 0 & 1 & 0 & 0 \\ 0 & 0 & 1 & 0 \\ 0 & 0 & 0 & 0 \end{bmatrix} \tag{15}$$

and E, F, G, $\bar{E}$, $\bar{F}$, $\bar{G}$, $E^*$, $F^*$, and $G^*$ are 4 x 4 matrices. The barred and starred matrices contain the initial stress and deformation

quantities and vanish if the initial state is a zero state. The starred quantities reflect the contribution of the square of the initial rotations on the behavior of the problem. Equation (14) may be applied to linear static stress analysis problems by setting the barred and starred quantities to zero and letting $\ddot{z} = 0$, applied to buckling problems by setting $\ddot{z} = e = 0$, and applied to prestressed vibration problems with $e = 0$, and assuming $z$ harmonic in time.

E. Boundary Conditions

In Sanders' nonlinear theory, the conditions to prescribe on the edge of a shell of revolution are

$$N_s \text{ or } U \qquad \hat{N}_{s\theta} \text{ or } V$$
$$\hat{Q}_s \text{ or } W \qquad M_s \text{ or } \phi_s \tag{16}$$

where $\hat{N}_{s\theta}$ and $\hat{Q}_s$ are the effective shear and transverse forces per unit length defined by

$$\hat{N}_{s\theta} = N_{s\theta} + (3R_\theta^{-1} - R_s^{-1})M_{s\theta}/2 + \underline{(N_s + N_\theta)\phi/2} \tag{17}$$

$$\hat{Q}_s = Q_s + M'_{s\theta}/r - \underline{\phi_s N_s - \phi_\theta N_{s\theta}} \tag{18}$$

Using the equilibrium equation (9) to eliminate $Q_s$ from equation (18) leads to

$$\hat{Q}_s = [(rM_s)' + 2M'_{s\theta} - r'M_\theta]/r - \underline{\phi_s N_s - \phi_0 N_{s0}} \tag{19}$$

Elastic restraints at the edge of a shell can be provided for by linearly relating the forces or moment to the appropriate displacements or rotation. Consequently, the boundary conditions may be given in the matrix form

$$\left[\bar{\Pi}\right]\begin{Bmatrix} N_s \\ \hat{N}_{s\theta} \\ Q_s \\ \Phi_s \end{Bmatrix} + \left[\bar{\Lambda}\right]\begin{Bmatrix} U \\ V \\ W \\ M_s \end{Bmatrix} = \ell \qquad (20)$$

where $\bar{\Pi}$ and $\bar{\Lambda}$ are 4x4 matrices and $\ell$ is a column matrix. The values of the elements of these matrices are determined by the conditions prescribed at the shell boundary. Procedures have been developed for independent boundary conditions of an uncoupled Fourier harmonic distribution. For the present case, however, simultaneous boundary conditions are imposed.

F. Ring Stiffeners

Circumferential ring stiffeners can be simulated at an arbitrary location along the shell. It is assumed that the ring has principal moments of inertia $I_{rx}$ and $I_{ry}$ about the centroidal axes which are perpendicular and parallel, respectively, to the axis of revolution. Further, the cross-sectional area, A, eccentricity, $\bar{e}$, and torsional constant, GJ, of the ring are specified. The basic problem is to determine the governing field equations of a ring that are compatible with Sander's shell equations.

Cohen[7] and Bushnell[8] have presented the generalized stiffness of rings. Weeks and Walz[9] illustrate a more thorough discussion when the centroid and shear center of the ring do not coincide. The above authors use the energy approach to derive the stiffness of the ring.

When the centroid and shear center are assumed to coincide and plane normal sections are assumed to remain plane and

normal during deformation, the ring strain energy is given by

$$\tilde{U}_r = \frac{r_c}{2} \int_0^{2\pi} \int_A \sigma_r \, (\bar{\varepsilon}_r - \alpha_T \, T) \, dA \, d\theta + \frac{1}{2} \frac{GJ}{r_c} \int_0^{2\pi} (\dot{\phi}_s + \frac{\dot{U}}{r_c})^2 \, d\theta \tag{21}$$

The hoop stress is defined to be

$$\sigma_r = E_r \, (\bar{\varepsilon}_r - \alpha_T \, T) \tag{22}$$

and the strain is defined by

$$\bar{\varepsilon}_r = \varepsilon_r - X \, k_x + Y \, k_y \tag{23}$$

The strain energy for the ring is therefore expressed:

$$\tilde{U}_r = \frac{r_c}{2} \int_0^{2\pi} \varepsilon_r^2 \, EA + k_x^2 \, EI_{ry} + k_y^2 \, EI_{rx} - 2 \, k_x \, k_y \, EI_{rxy} + \frac{GJ}{r_c} (\dot{\phi}_s + \dot{U}_r/r_c)^2 + 2 \, [\varepsilon_r \, N_r^T - k_x \, M_y^T + k_y \, M_x^T] \, d\theta \tag{24}$$

Where, the thermal loads are defined by

$$N_r^T = - \int_A E_r \, \alpha_r \, T \, dA \tag{25a}$$

$$M_y^T = - \int_A E_r \, \alpha_r \, X \, dA \tag{25b}$$

$$M_x^T = - \int_A E_r \, \alpha_r \, Y \, dA \tag{25c}$$

and the strain displacement relations are

$$\left.\begin{aligned} \varepsilon_r &= \dot{V}_r/r_c + W_c/r_c + \tfrac{1}{2}(\phi_{\theta r}^2 + \phi_{\theta r}^2) \\ k_x &= \dot{\phi}_{\theta r}/r_c \qquad ; \qquad k_y = -\dot{\phi}_{\theta r}/r_c \oplus \phi_s/r_c \\ \gamma_{sr} &= (\dot{W}_r - V_r)/r_c \\ \phi_{\theta r} &= \dot{U}_r/r_c \end{aligned}\right\} \tag{26}$$

The kinetic energy of a discrete ring is given by

$$T_r = \rho_r\left(\frac{r_c}{2}\right)\int_0^{2\pi} [A\,(U_{r,t}^2 + V_{r,t}^2 + W_{r,t}^2) + I_p\,\phi_{s,t}^2 + I_x\,\phi_{\theta r,t}^2 + I_y\,\phi_{\theta r,t}^2 - 2\,I_{xy}\,\phi_{\theta r,t}\,\phi_{\theta r,t}]\,d\theta \tag{27}$$

From the variational principle, the derivatives with respect to each of the fundamental variables will develop the stiffness and mass matrices.

The stiffness matrix is defined for a given Fourier harmonic, n, response by

$$G = \frac{E}{r_c^2}\begin{bmatrix} \frac{n^2}{r_c^2}(n^2 I_x + \frac{GJ}{E}) & \frac{n^4}{r_c^2} I_{xy} & \frac{n^3}{r_c^2} I_{xy} & -\frac{n^2}{r_c}(I_x + \frac{GJ}{E}) \\ & A + \frac{n^4 I_y}{r_c^2} & n(A + \frac{n^2}{r_c^2} I_y) & -\frac{n^2}{r_c} I_{xy} \\ & \text{Symmetric} & n^2(A + \frac{I_y}{r_c^2}) & -\frac{n^2}{r_c} I_{xy} \\ & & & I_x + n^2 \frac{GJ}{E} \end{bmatrix} \tag{28}$$



AE-14

not dimensionally correct

Mass matrix does not agree with stiffness layout matrix

and the mass matrix

$$\bar{\mu} = \frac{\rho}{r_c} \begin{bmatrix} r_c^2 A + n^2 I_y & n I_{xy} & n^2 I_{xy} & 0 \\ & r_c^2 A + I_x & n I_x & 0 \\ & \text{Symmetric} & r_c^2 A + n^2 I_x & 0 \\ & & & r_c^2 (I_x + I_y) \end{bmatrix} \begin{matrix} u \\ v \\ w \\ \phi_s \end{matrix} \qquad (29)$$

The displacements and the rotation of the ring are related to a point on the shell's reference surface at the ring attachment by

$$\left.\begin{aligned} U_r &= U - e_1 \phi_s \\ V_r &= -e_2/r_c\, U + V\,(1 + e_1/r_c) - e_1/r_c\, W \\ W_r &= W + e_2 \phi_s \\ \phi_r &= \phi_s \end{aligned}\right\} \qquad (30)$$

where the eccentricities of the ring to the shell are $e_1$ and $e_2$ in the X and Y direction, respectively.

For prismatic rings the force-displacement relations are noted to be

$$\left.\begin{aligned} N_{\theta_r} &= \frac{EA}{r_c}(V_r' + W_r) \\ M_{\theta_r} &= \frac{EI}{r_c^2}(-W_r'' + V_r') \\ M_{t_r} &= \frac{GJ}{r_c}(-W_r' - U_r'/r_c) \end{aligned}\right\} \qquad (31)$$

With the definition of $\phi_s = W_r'$, and by substituting equation (28) which represents the stiffness into equation (14), the ring can be easily introduced into the overall equilibrium of the shell.

## III METHOD OF SOLUTION

### A. Fourier Expansions

The crux of the method used here to solve the nonlinear field equations is the elimination of the independent variable $\theta$ by expanding all dependent variables into sine or cosine series in the circumferential direction. Only loading and initial conditions that are symmetric about a datum meridian plane will be considered. Thus, the variable $\phi_s$ can be expressed in the form*

$$\phi_s = \frac{\sigma_o}{E_o} \sum_{n=0}^{\infty} \phi_s^{(n)} \cos n\theta \tag{32}$$

where $\sigma_o$ is a reference stress level, $E_o$ is a reference elastic modulus, and the nondimensional series coefficient $\phi_s^{(n)}$ is a function of the independent variables s and T. Similar series expansions can be made for the remaining dependent variables.

### B. Modal Uncoupling

In order to eliminate the independent variable $\theta$ from the problem, and convert the partial differential equations to sets of uncoupled partial differential equations, the nonlinear terms are treated as known quantities or pseudo loads. Since every nonlinear term is the product of two Fourier series, each product can be reduced to a single trigonometric series wherein the coefficient is itself a series. For example, using equation (32), $\phi_s^2$ can be expressed as

$$\phi_s^2 = \left(\frac{\sigma_o}{E_o}\right)^2 \sum_{m=0}^{\infty} \sum_{n=0}^{\infty} \phi_s^{(m)} \phi_s^{(n)} \cos m\theta \cos n\theta \tag{33}$$

*Theoretically, the complete Fourier series including both the sine and cosine expansions should be used because of the possibility of "odd" displacements occurring under "even" loads, i.e., a bifurcation phenomenon. This aspect is not considered here for the nonlinear case.

See Appendix A*

Since

$$\cos m\theta \cos n\theta = \frac{1}{2}[\cos (m-n)\theta + \cos (m+n)\theta] \tag{34}$$

equation (18) can be given in the form

$$\phi_s^2 = \frac{\sigma_o}{E_o} \sum_{n=0}^{\infty} \beta_s^{(n)} \cos n\theta \tag{35a}$$

where

$$\beta_s^{(n)} = \frac{\sigma_o}{2E_o} \sum_{i=0}^{\infty} \phi_s^{(i)} [\eta\, \phi_s^{(i+n)} + \mu\, \phi_s^{(|i-n|)}] \tag{35b}$$

ABSOLUTE VALUE

with

$$\eta = \begin{cases} 0 \text{ for } n = 0 \\ 1 \text{ for } n > 0 \end{cases}, \quad \mu = \begin{cases} 1 \text{ for } i \neq n \\ 2 \text{ for } i = n \end{cases}$$

Similar series expressions can be derived for the other nonlinear terms in equations (5), (8), (17), and (18b). They are

$$\left.\begin{aligned} \phi_\theta^2 &= \frac{\sigma_o}{E_o} \sum_{n=0}^{\infty} \beta_\theta \cos n\theta \\ \phi^2 &= \frac{\sigma_o}{E_o} \sum_{n=0}^{\infty} \beta \cos n\theta \\ \phi_s\phi_\theta &= \frac{\sigma_o}{E_o} \sum_{n=1}^{\infty} \beta_{s\theta} \sin n\theta \\ \phi_s N_s &= \sigma_o h_o \sum_{n=0}^{\infty} \eta_{ss} \cos n\theta \\ \phi_\theta N_{s\theta} &= \sigma_o h_o \sum_{n=0}^{\infty} \eta_{\theta s} \cos n\theta \\ \phi N_s &= \sigma_o h_o \sum_{n=1}^{\infty} \eta_s \sin n\theta \end{aligned}\right\} \tag{35c}$$



AE-17

$$\left.\begin{aligned} \phi N_\theta &= \sigma_o h_o \sum_{n=1}^{\infty} \eta_\theta \sin n\theta \\ \phi_\theta N_0 &= \sigma_o h_o \sum_{n=1}^{\infty} \eta_{00} \sin n\theta \\ \phi_s N_{s\theta} &= \sigma_o h_o \sum_{n=1}^{\infty} \eta_{s\theta} \sin n\theta \end{aligned}\right\} \qquad (35c)$$

where $h_o$ is a reference thickness.

As a result of the trigonometric series expansions, there is one set of governing equations for each value of n considered; when only the linear terms are considered the sets are uncoupled. The presence of the nonlinear terms couples the sets through terms like $\beta_s^{(n)}$ as given by equation (35). However, by treating the nonlinear terms as known quantities and grouping them with the load terms, the sets of equations become uncoupled.

C. Spatial Finite Difference Formulation

Let the shell meridian be divided into K - 1 equal increments, and denote the end of each increment or station by the index i. Thus, i = 1 corresponds to the initial edge of the shell and i = K corresponds to the final edge. One fictitious station is introduced off each end of the shell at i = 0 and i = K + 1.

Let the first and second derivatives of z at station i be approximated by

$$z_i' = (z_{i+1} - z_{i-1})/2\Delta \qquad (36a)$$

$$z_i'' = (z_{i+1} - 2z_i + z_{i-1})/\Delta^2 \qquad (36b)$$



AC-1A

where Δ is the nondimensional distance between stations. Substituting equations (36a) and (36b) into equation 14 leads to

$$A_i z_{i+1} + B_i z_i + C_i z_{i-1} = g_i + 2\Delta\bar{\mu}_i (\partial^2 z/\partial t^2)_i \tag{37a}$$

where

$$\begin{aligned} A_i &= 2E_i/\Delta + F_i \\ B_i &= -4E_i/\Delta + 2\Delta G_i \\ C_i &= 2E_i/\Delta - F_i \\ g_i &= 2\Delta e_i \quad ; \quad \bar{\mu}_i = \nu I \end{aligned} \tag{37b}$$

and i = 1, 2 . . . K to insure equilibrium over the total length of the shell.

At the boundaries equation (20) must be satisfied. Thus, substituting equation (36a) into equation (14) leads to

$$\frac{1}{2\Delta}\Omega_1 H_1 z_2 + (\Omega_1 J_1 + A_1) z_1 - \frac{1}{2\Delta}\Omega_1 H_1 z_0 = \ell_1 - \Omega_1 f_1 \tag{38a}$$

at the initial edge, and

$$\frac{1}{2\Delta}\Omega_K H_K z_{K+1} + (\Omega_K J_K + A_K) z_K - \frac{1}{2\Delta}\Omega_K H_K z_{K-1} = \ell_K - \Omega_K f_K \tag{38b}$$

at the final edge.

For many cases, a shell structure comprised of composite elements develop discontinuity stresses near their juncture point. For example, a discontinuity in the membrane stress resultants will occur at the juncture of a cylindrical and spherical shell. In order to more accurately determine the stress distribution near these discontinuities, the mesh distribution must be finer than those areas away from the juncture.

A variable mesh spacing is represented at station i

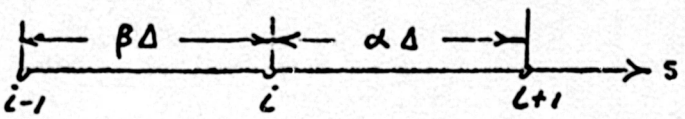


Let $\beta\Delta$ = Ratio $(i-1)\Delta_L$ and $\alpha\Delta$ = Ratio $(i)\Delta_L$, where $\Delta_L$ is the mesh spacing at the last station. From a Taylor's series expansion

$$Z_{i+1} = Z_i + \alpha\Delta\, Z_i' + \frac{(\alpha\Delta)^2}{2!} Z_i'' + \frac{(\alpha\Delta)^3}{3!} Z_i''' + \cdots \tag{39a}$$

$$Z_{i-1} = Z_i - \beta\Delta\, Z_i' + \frac{(\beta\Delta)^2}{2!} Z_i'' - \frac{(\beta\Delta)^3}{3!} Z_i''' + \cdots \tag{39b}$$

Multiplying the first by $\beta^2$ and the second by $\alpha^2$ we obtain for the first derivative

$$Z_i' = \frac{1}{(\beta+\alpha)\alpha\beta\Delta} \left[\beta^2 Z_{i+1} + (\alpha^2 - \beta^2) Z_i - \alpha^2 Z_{i-1}\right] \underbrace{- \frac{\alpha\beta\Delta^2}{6} Z_i'''}_{O(\Delta^2)} \tag{40}$$

and for the second derivative

$$Z_i'' = \frac{2}{(\alpha+\beta)\alpha\beta\Delta^2} \left[\beta Z_{i+1} - (\beta+\alpha) Z_i + \alpha Z_{i-1}\right] \underbrace{- \frac{2(\alpha-\beta)\Delta}{3!} Z_i'''}_{O(\Delta)} \tag{41}$$

Since the error term in the second derivative is of order $\Delta$, a variable mesh spacing through the discontinuity should not take place. Errors will occur at the juncture of the variable mesh. If the bending is low in these regions, no significant error in the solution should occur.

Lab. No. 173.3
January 4, 1973

# A COMPUTER PROGRAM for the EVALUATION of SPECTRUM ACCELERATION USING FFT TECHNIQUES

By
Ray Bieber

Anamet Laboratories, Inc.
P. O. Box 631
San Carlos, California 94071

AE.21

ANALYTICAL STRUCTURES, INC.
P.O. BOX 831, SAN CARLOS, CALIFORNIA 94070

# I Introduction

In displaying the transient response of a structure to time-dependent loading, there are two primary choices available. One is to use the actual time history or "signature" of the measured or predicted quantity as the best index of the response characteristics. Secondly, some type of spectral representation which shows the predominate frequency content of the signal can be constructed. The use of the FFT for spectrum transient ground acceleration evaluation had been earlier proposed by Citerley[1]. In the present study the computation of an acceleration spectrum from transient data using the Fast Fourier Transform (FFT) algorithm is presented. The end result is a Fortran IV Digital Computer program for implementing the solution. The program was developed for use as a post-processor in analyzing the displacement output from a shell of revolution code; however it can also be used as a general purpose signal analysis routine.



CE-22

Anamet Laboratories, Inc.

P.O. BOX 831, SAN CARLOS, CALIFORNIA 94070

## II Analysis

### A. Continuous Solution

The acceleration spectrum equations will be shown in "continuous" form and then restated for digital computation. For discussion purposes, the signal to be analyzed is a finite acceleration time history $\ddot{X}_o(t)$, continuous in the interval $0 \leq t \leq T$, and identically zero outside. The frequency content of $\ddot{X}_o(t)$ in a narrow range centered at frequency $\omega_n$ can be examined by considering the solution of,

$$\ddot{X}(t) + 2\,\xi\,\omega_n\,\dot{X}(t) + \omega_n^2\,X(t) = -\,\ddot{X}_o(t) \tag{1}$$

which is the response of a lightly damped ($\xi \ll 1.0$) single-degree-of-freedom spring-mass system to base acceleration, $\ddot{X}_o(t)$. The solution of (1) for the acceleration response, $\ddot{X}(t)$, can be expressed in integral form as,

$$\begin{aligned} \ddot{X}(t) &= \int_0^t h\,(t-\tau)\,\ddot{X}_o(\tau)\,d\tau \\ &= \omega_n \int_0^t e^{-\xi\omega_n(t-\tau)} \sin\,[\omega_n(t-\tau)]\,\ddot{X}_o(\tau)\,d\tau \end{aligned} \tag{2}$$

The above solution assumes zero initial conditions in $X$ and $\dot{X}$.

The acceleration spectrum of $\ddot{X}_o$ will be defined as the maximum absolute value of $\ddot{X}$, i.e.

$$\begin{aligned} S_{\ddot{X}_o}(\omega_n;\xi) &= \mathrm{MAX}\ \{\ \mathrm{ABS}\ [\ \ddot{X}(t)\ ]\} \\ &= \mathrm{MAX}\ \{\ \mathrm{ABS}\ [\ \omega_n \int_0^t e^{-\xi\omega_n(t-\tau)} \sin\,\omega_n(t-\tau)\,\ddot{X}_o(\tau)d\tau]\} \end{aligned} \tag{3}$$

The argument $(\omega_n;\xi)$ denotes that $S\ddot{X}_o$ is a function of $\omega_n$ and parameter, $\xi$. The selected values of $\xi$ will usually be on the order of 0, .05, - - - .20.

Defining the Fourier transform of X(t) as,

$$X(i\omega) = \int_0^\infty \ddot{X}(t)\, e^{i\omega t}\, dt \tag{4}$$

then a transform solution for $\ddot{X}$ can be obtained. Taking the transform of both sides of (2) and applying the well-known convolution theorem, the following is obtained,

$$\ddot{X}(i\omega) = h(i\omega)\, \ddot{X}_o(i\omega)$$

$$\equiv \frac{\omega^2\, \ddot{X}_o(i\omega)}{\omega_n^2 - \omega^2 + 2\,\xi\,\omega_n\,\omega i} \tag{5}$$

Taking the inverse Fourier Transform of both sides,

$$\ddot{X}(t) = \ddot{X}^{-1}(i\omega) = \left[ \frac{\omega^2\, \ddot{X}_o(i\omega)}{\omega_n^2 - \omega^2 + 2\,\xi\,\omega_n\,\omega i} \right]^{-1} \tag{6}$$

where, the inverse transform is defined as

$$X(t) = X^{-1}(i\omega) = \frac{1}{\pi}\int_0^\infty X(i\omega)\, e^{-i\omega t}\, d\omega \tag{7}$$

Thus in terms of Fourier transforms the acceleration spectrum can be expressed,

$$S\ddot{X}_o(\omega_n;\zeta) = \mathrm{MAX}\ \{\ \mathrm{ABS}\ [\ \ddot{X}(t)\ ]\ \}$$

$$= \mathrm{MAX}\ \{\ \mathrm{ABS}\ \left[\frac{1}{\pi}\int_0^\infty \frac{\omega^2\, \ddot{X}_o\,(i\omega)\, e^{-i\omega t}\, dt}{\omega_n^2 - \omega^2 + 2\,\xi\,\omega_n\, i}\right]\} \tag{8}$$

B. Digital Solution

The most common method of solving for $\ddot{X}(t)$ is by numerical integration of equation (2), e.g. Simpson's rule. With the development of the Fast Fourier Transform (FFT) Algorithm, (see for example Ref. 2), it can be shown that it is numerically more efficient to use the transform form of the solution i.e. equation (6). Two digital solutions of the acceleration spectrum will be presented; one where the displacement signal $X_o(t)$ is given and the other where the acceleration $\ddot{X}_o(t)$ is given.

Using the notation and the definitions from Ref. 3, the FFT of the digital time series $X(t)$, $t=0, 1, - - - -, N-1$, is given by

$$X(\hat{t}) = \sum_{t=0}^{N-1} X(t) \; e^{\frac{2\pi i t \hat{t}}{N}} \tag{9}$$

Notice that the units of frequency are now Hz rather than Rad/sec as in the previous section i.e.

$$\omega = 2\pi f \tag{10a}$$

$$\omega_n = 2\pi f_n \tag{10b}$$

The time interval is $\Delta t = T/N$ and the frequency interval is $\Delta f = 1/T = 1/N\Delta t$ The highest frequency is $N\Delta f = 1/\Delta t$ which is the digital sampling rate. Thus there are an equal number, N, time ordinates and frequency ordinates. The inverse FFT of $X(\hat{t})$ is given by,

$$X(t) = \frac{1}{N} \sum_{\hat{t}=0}^{N-1} X(\hat{t}) \cdot e^{-\frac{2\pi i t \hat{t}}{N}} \tag{11}$$

One additional discrete transform theorem (Ref. 3) for finite difference derivatives is needed.

$$\sum_{t=0}^{N-1} \frac{\Delta X(t)}{\Delta t} \, e^{\frac{2\pi i t \hat{t}}{N}} = \frac{1}{\Delta t} \left(e^{\frac{-2\pi i \hat{t}}{N}} - 1\right) X(\hat{t}) \tag{12}$$

$$\text{where:} \quad \Delta X(t) = X(t+1) - X(t) \tag{12a}$$

Thus (12) gives the Fourier transform of the forward difference derivative of the function, X(t).

The discrete transform solution of equation (6) can now be written,

$$\ddot{X}(t) = \frac{1}{N} \sum_{\hat{t}=0}^{N-1} \frac{f^2 \, \ddot{X}_o(\hat{t}) \, e^{\frac{-2\pi i t \hat{t}}{N}}}{f_n^2 - f^2 + 2\zeta f_n f i} \tag{13}$$

$$\text{where:} \quad f = \hat{t}\Delta f, \quad \hat{t} = 0, 1, - - - -, N-1 \tag{13a}$$

$$f_n = n\Delta f, \qquad 0 \leq n \leq N-1$$

Substituting for f & $f_n$,

$$\ddot{X}(t) = \frac{1}{N} \sum_{\hat{t}=0}^{N-1} \left[\frac{\hat{t}^2}{n^2 - \hat{t}^2 + 2\zeta n \hat{t} i}\right] \ddot{X}_o(\hat{t}) \, e^{\frac{-2\pi i t \hat{t}}{N}} \tag{14}$$

The computational procedure for solving (14) is:

(1) Solve for $\ddot{X}_o(\hat{t})$ given the input signal, $\ddot{X}_o(t)$

(2) Multiply $\ddot{X}_o(\hat{t})$ by the complex filter function in the brackets

(3) Take the inverse transform of the complex product obtained in step (2).

For the case where the displacement of the signal is given rather than the acceleration, the derivative theorem of (12) is applied i.e.

$$\ddot{X}_o(\hat{t}) = \sum_{t=0}^{N-1} \frac{\Delta \dot{X}(t)}{\Delta t} \, e^{\frac{2\pi i t \hat{t}}{N}} \qquad (15)$$

$$= \frac{1}{\Delta t^2} \left(e^{\frac{-2\pi i \hat{t}}{N}} - 1\right)^2 X(\hat{t})$$

Thus the computational procedure for solving (14), given the displacement, $X_o(t)$, is as follows:

(1) Solve for the transform, $X_o(\hat{t})$

(2) Compute $\ddot{X}_o(t)$ by (15)

(3) Multiply $\ddot{X}_o(t)$ by the complex filter function according to (14)

(4) Take the inverse transform of the complex product obtained in step (3).

The acceleration spectrum $S_{\ddot{X}_o}(\omega_n;\zeta)$ is easily solved from the definition, once the acceleration $\ddot{X}(t)$ is known.

Inland Laboratories, Inc.

P.O. BOX 831, SAN CARLOS, CALIFORNIA 94070

## III Computer Program

A computer program is described for evaluating the acceleration spectrum given either a displacement or acceleration signal. An arbitrary number of functions can be analyzed. The damping values and spectral frequencies are specified in the input data.

The FFT routine employed in computing the discrete transforms is that of Ref. 3*. The program will accomodate up to a 3-D complex function. Since the FFT technique relies on the length of the time series being of the form $N=2^n$, where n is an integer, the method of "filling out" with zeroes will be used. For example if a time series of length 1000 is given, then 24 zeros values will be added to form a new series of length $N = 2^{10} = 1024$.

The computer program is written in FORTRAN IV and is listed in Appendix A. A schematic of the solution for one input signal is shown in Fig. 1. The input time histories (displacement or acceleration) are analyzed sequentially. The input data format for each signal is given below.

Card 1 - Control Card

Format (3I5)

| Col. | | |
|---|---|---|
| 1-5 | IKIND | (1 for Displacement, 2 for Acceleration) |
| 6-10 | ND | (Unit Number of tape or drum for use in copying input or output data) |
| 11-15 | NL | (Length, number of data points in input signal) |

---

*Other standard routines are available through SHARE.

Card 2 - Control Card

Format (6F10.0)

| Col. | | |
|---|---|---|
| 1-10 | DELT | (Input record time interval, sec.) |
| 11-20 | ZETA | (Damping ratio, nondimensional) |
| 21-30 | FLO | (Acceleration spectrum lowest frequency required, Hz) |
| 31-40 | FHI | (Highest frequency required, Hz) |
| 41-50 | DF | (Frequency interval, Hz) |
| 51-60 | CONST | (Scale factor) |

Card 3, - - -, N Data Cards

Format (8F10.0)

The card image form of the time series data can easily be changed to accommodate other formats. Also the time series data can be supplied on Unit ND via external control cards, so that handling of bulky cards is avoided.

END Card

Format (I5)

| Col. | | |
|---|---|---|
| 1-5 | 99999 | (End of Data) |

This card is supplied after all of the input signatures have been read and signals the end of the data deck.

In using the program and interpreting the spectral results, it must be remembered that the highest frequency component in the data to be analyzed must be less than 1/2 the highest FFT frequency, ($f_{max} = \frac{1}{\Delta t}$). If this is not the case, digital band-pass filtering of the raw data must be performed prior to spectral analysis. The latter can be easily accomplished using "autoregressive" or "moving average" techniques.

Agbabian Laboratories, Inc.
P.O. BOX 831, SAN CARLOS, CALIFORNIA 94070

Figure 1 Flow Diagram for Calculation of Acceleration Spectrum for Displacement or Acceleration Input Record

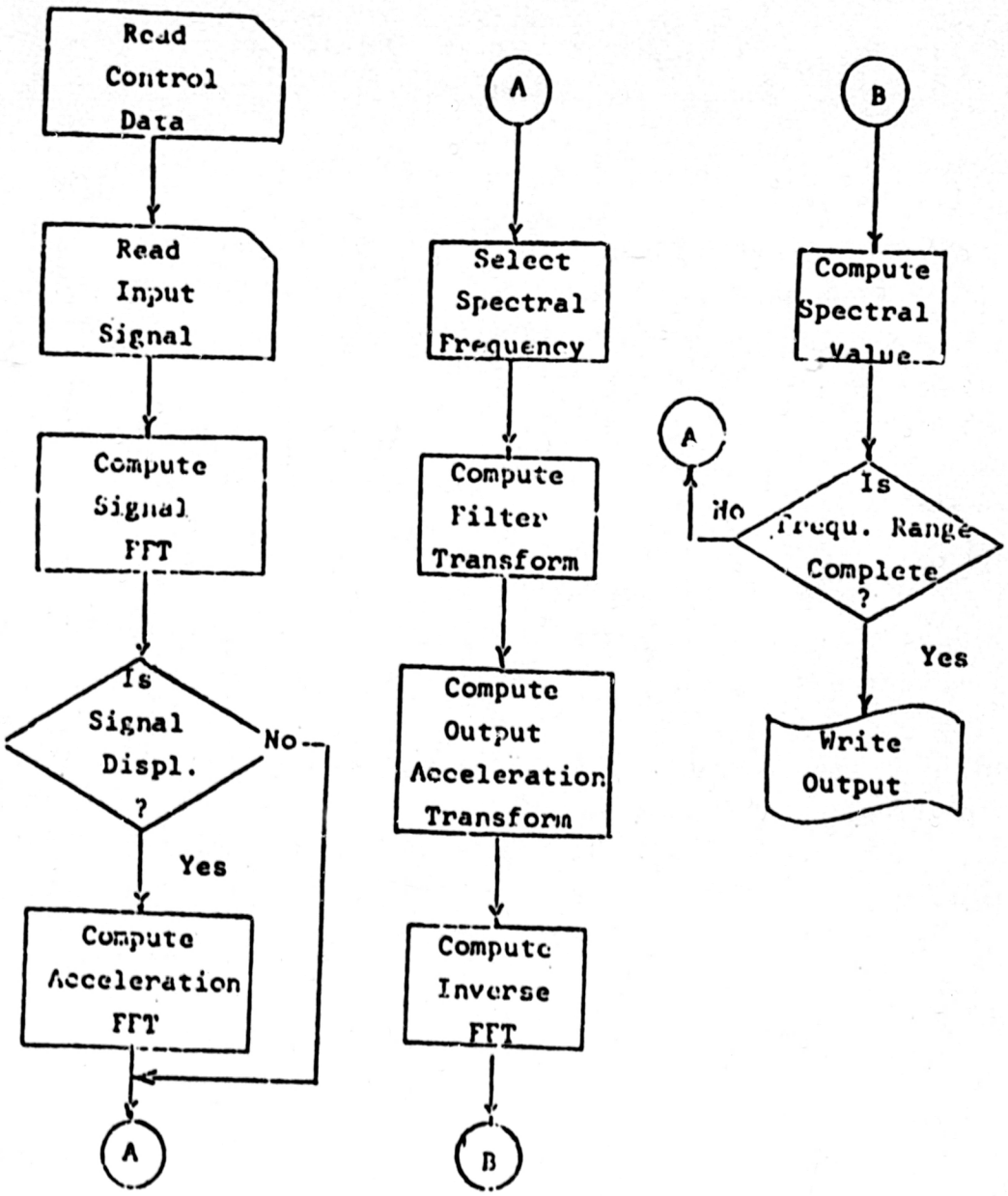

Anamet Laboratories, Inc.

P.O. BOX 931, SAN CARLOS, CALIFORNIA 94070

## References

1. Citerley, R.L., Estimation of Ground Acceleration from Spectral Data, Anamet Report No. 470.259, April 1970.

2. Bergland, G.D., A Guided Tour of the Fast Fourier Transform, IEEE Transactions on Audio and Electroacoustics, June 1967.

3. Gentleman, W.M. and Sande, G., Fast Fourier Transforms - For Fun and Profit, Proceedings - Fall Joint Computer Conference, 1966.

## APPENDIX C'

## The Design of a Thin Shell Nuclear Containment Vessel for Seismic Loading

by J. Hagstrom

This article is contained in the Journal of Engineering for Industry, August 1972, pages 803-806.

# APPENDIX D'

## Mass Loading Effects on Vibration of Ring and Shell Structure

SD 68-29

# MASS-LOADING EFFECTS ON VIBRATION OF RING AND SHELL STRUCTURES

(CONTRACT NAS8-20019, PHASE III)

February 1968


Prepared by

S. Y. Lee
S. S. Tang
J. G. Liycos

Approved by

S. Y. Lee, Project Engineer

F. C. Hung, Program Manager

Structures & Design Dept., Research, Engineering & Test

SPACE DIVISION
NORTH AMERICAN ROCKWELL CORPORATION

## ABSTRACT

Efficient methods for predicting the effects of attached masses on the vibration characteristics of ring and shell structures were developed and substantiated with experimental data. Analytically, the series expansion technique was used in solving the mass-loaded shell problem, while both the finite-element and transfer-matrix methods were employed in the analysis of mass-loaded ring structures. Experimentally, aluminum ring and shell structures loaded with discrete masses were excited by a electrical induction force, and the vibratory motion was measured by an automatically revolving proximity gage. The influences of the masses of the exciter and of the instrumentation, thus, were eliminated. Response data were obtained with miniature accelerometers and with a proximity gage for comparison purposes. The studies show, in addition to the amplitude changes of the local vibration response caused by the addition of the discrete masses, the frequency shifts, the change of modal behavior, and the transmissibility characteristics resulting from the increased discrete mass on the structure. The results show (1) that the response attenuation for the first mode was somewhat similar to the procedure currently recommended by NASA/MSFC for predicting the amplitude reduction of the local vibration response of unloaded structure to account for the influence of the addition of the mass; (2) that for higher modes, much more amplitude reductions were found, and the rate of amplitude reduction progressed very rapidly; and (3) that the transmissibility characteristics in a function of normal modes, indicated some differences for beams, plates, honeycomb plates, rings, and shells.

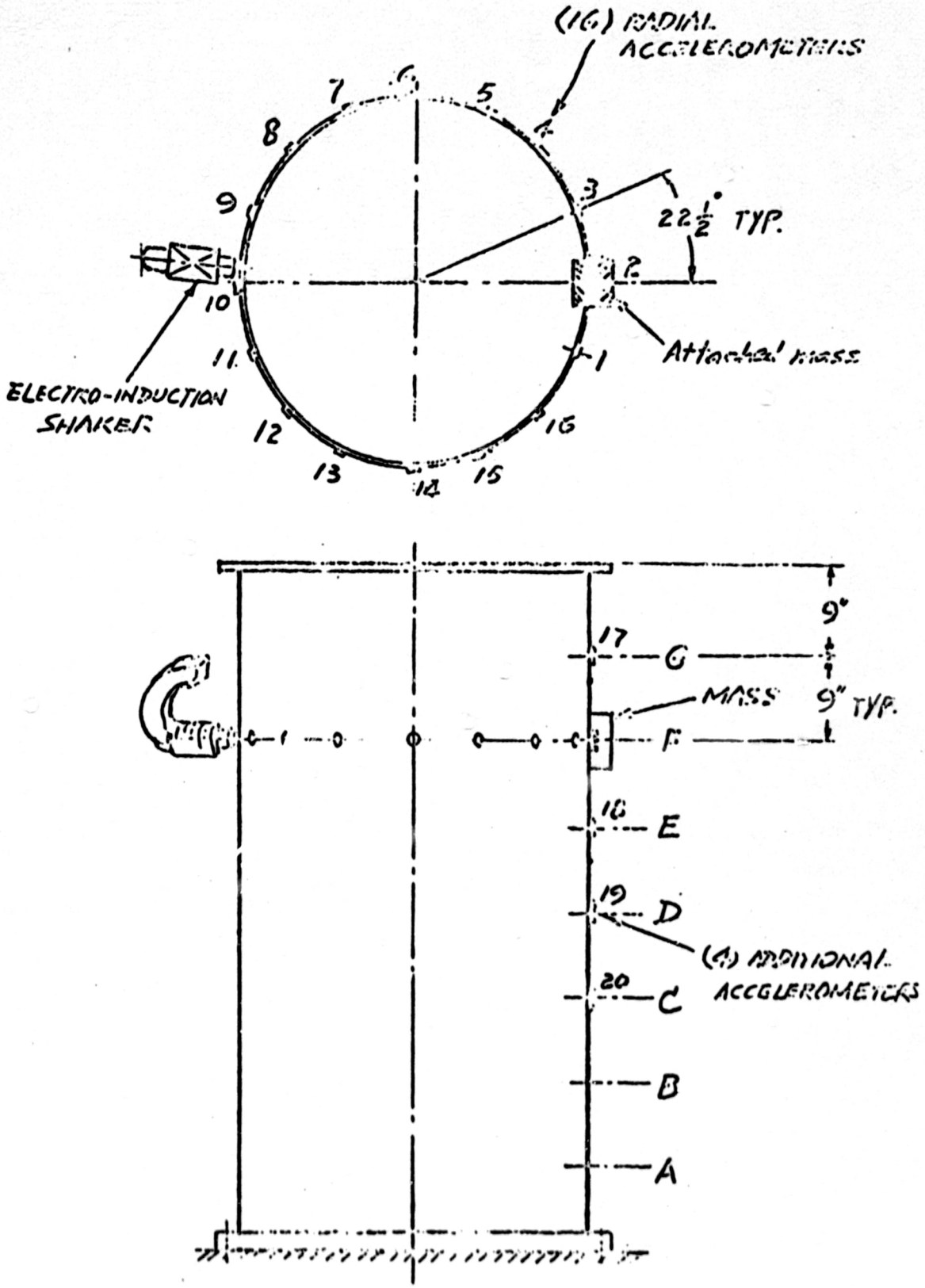


Figure 13. Accelerometers Set-up for Vibration Test of Mass-Loaded Shell

## 7.0 CONCLUSIONS

The analytical and experimental studies of the mass-loading effects on vibration of rings and shells can be summarized as follows:

1. Efficient methods have been developed for analyzing vibration of mass-loaded ring and shell structures.

2. Analytical results closely agreed with test data.

3. Frequency-shifts for mass-loaded rings and shells differed somewhat from those previously obtained in the Phases I and II of this program for the cases of beams and plates. Because of the motion of the mass interacted with the two- or three-dimensional motions of the support structures, the effect of mass loading on rings and shells caused a decrease in natural frequencies; however, for the higher modes, the frequency shifts became less significant as the attached mass increases. This information was presented in this report in the form of equations, tables, plots, and nondimensional graphs for various applications.

4. Transmissibilities and attenuations followed a trend similar to that of beams and plates, but possessed special characteristics. The results followed the equation $y = A + \frac{B}{X^n}$ which was previously established in Phases I and II of this program. The coefficients A, B, and n can be determined from the transmissibility plots in conjunction with firing test data and some consideration for design safety.

5. Mass loading also caused changes in mode shapes and disappearance of some modes at the mass mounting location; however, these phenomena of rings and shells deviated from that of beams and plates and were demonstrated by test data and computer solutions in this report.

6. The free vibration characteristics of mass-loaded shells can be solved analytically by the Fourier series-expansion technique.

which gives closed-form and nearly exact solution. This method required the use of four summations of the m n i j terms instead of only two summations of m n terms to describe the interacted motion.

7. Transfer matrix methods were efficient in calculating the lower frequencies of ring structures, while the finite-element method was good for both lower and higher frequencies. The transfer matrix method, however, offered a simple direct solution which provided a step-by-step insight into the solution and was helpful in the study of response characteristics.

8. The developed experimental and instrumentation techniques permitted continuous plotting of mode shapes and produced meaningful data for immediate evaluation during the test.

9. Sufficient data had been obtained for smaller mass ratios to better define the mass-loading phenomena.

As a general conclusion to the study, the trend of mass-loading effects on vibration of ring and shell structures has been established and the prediction methods have been developed; however, some refined studies and investigations for applications are needed and recommended as follows:

1. Refine the closed-form exact-solution technique for shell vibration analysis.

2. Further define the analysis of mass-loading effects on modal characteristics of shell structures.

3. Investigate the finite-element technique for obtaining an approximate solution for shell vibration.

4. Apply results to solve bracketry problems, definition of support structures, design of local structures, and test and evaluation of components.

5. Further refine the experimental technique.

6. Simplify the analytical solution, and reduce the mathematical complexity for further development in the definition of the basic mass-loading mechanism.

7. Extend the developed method to solve vibration problems of complicated shell structures loaded with bulkheads, propellants, ring frames, longerons, and a variety of discrete masses.